



Signal processing Aspects of the Sample Clock Frequency Offset Scheme for the SKA1 Mid Telescope Array

Brent Carlson^{*(1)}, Thushara Gunaratne⁽¹⁾, and Mid.CBF Team⁽¹⁾⁽²⁾

(1) National Research Council Canada, National Science Infrastructure, P.O. Box 248, Penticton, BC, Canada V2A 6J9

(2) MDA Systems Ltd., 13800 Commerce Parkway, Richmond, BC, Canada V6V 2J3

Abstract

In the proposed sample clock frequency offset (SCFO) scheme, the received signals at *each* antenna of the Square Kilometre Array Mid Telescope Array are sampled at slightly *different* sample rates. Subsequently, these sampled sequences are digitally re-sampled to a common sample rate prior to channelization and correlation/beamforming. In this paper, the signal processing aspects of the SCFO scheme as it relates to the correlator and beamformer (CBF) of the SKA1 Mid Telescope are discussed. Here, it is shown that sample clock-related self-interference and out-of-band interference decorrelates improving the quality of correlated/beamformed results.

1. Introduction

The Square Kilometre Array (www.skatelescope.org), will be the next generation centimeter wave synthesis array telescope. It is in its final stages of its design phase and one of the main design objectives is to have dynamic range of order $1:10^6$ to 10^7 in the synthesized sky images [1,2]. The self-interference and spectral artifacts generated due to sampling may hinder achieving this objective.

Conventionally in synthesis array telescopes, when observing a particular frequency band, a sample clock derived from a unique coherent source is used to sample the received signal at each antenna. Hence, self-interference due to sample clock harmonics and those spectral artifacts introduced by interleaved samplers appear in the *same frequency* of the observation band for every received signal for all antennas. Also, for all sampled sequences, out-of-band signals including RFI, alias into the *same frequencies* in the observation band. Therefore, in the correlator these undesired spectral components correlate and in the beamformer, add coherently.

If *each* of the received signals is sampled at a unique rate, all the harmonics of the different sample clocks (except for those appearing at DC for Nyquist zone 1; for Nyquist zone 2 this is not the case) appear at different frequencies. Similarly, out-of-band interference is aliased into different frequencies in the received band. As shown later in this paper, even though the sampled sequences at different rates get digitally resampled into a common rate, self-

interference and aliased out-of-band interference remain at different frequencies and therefore, do not correlate in the correlator and do not add coherently in the beamformer. Note that the proposed sample clock frequency offset (SCFO) scheme also relaxes the transition-band and stop-band requirements of analog anti-aliasing filters in the receivers, because aliased components of these do not correlate or add coherently.

This paper is organized as follows. In Section 2, sampling clock-related distortions in samplers are briefly reviewed. In Section 3, the concept of the SCFO is illustrated with diagrams. The simulation results of a model implementation of the SCFO scheme in the Mid.CBF is given in Section 4. The conclusions and extension of the SCFO scheme are discussed in Section 5.

2. Sample Clock Related Distortions in Sampling

A stable clock is an essential requirement for a sampler in high sensitivity radio telescope such as the SKA1 Mid Array. However, due to non-idealities in the clock synthesizer, there can be relatively strong undesired additional components (i.e. clock spurs not synchronous with the sample clock frequency) contaminating clock phase. As shown in [3], spurs in the sample clock cause images of the input signal to alias into the sampled-signals causing spectral confusion. Also, in time-interleaved samplers, despite higher sample rate performance, due to the inherent time and gain mismatches in different arms of the sampler, the sampled signals are distorted by combinations of aliasing images of the input spectrum [4,5]. Note that the orientation of the aliased images in the sampled spectrum is related to the sampling clock frequency.

3. The Concept of the SCFO Scheme

A sampling scenario with the proposed SCFO scheme, where the desired signal is in Nyquist zone-1, is illustrated in Figure 1. The spectrum of the input signal to the sampler is shown in Figure 1-(a). As shown there, in addition to the desired wideband signal, there is an out-of-band signal at F_I where power leaks through the anti-aliasing filter. The spectra of the three corresponding sampled sequences at F_{S1} , F_{S0} and F_{S2} , are shown in Figure 1-(b), (c) and (d), respectively. Note

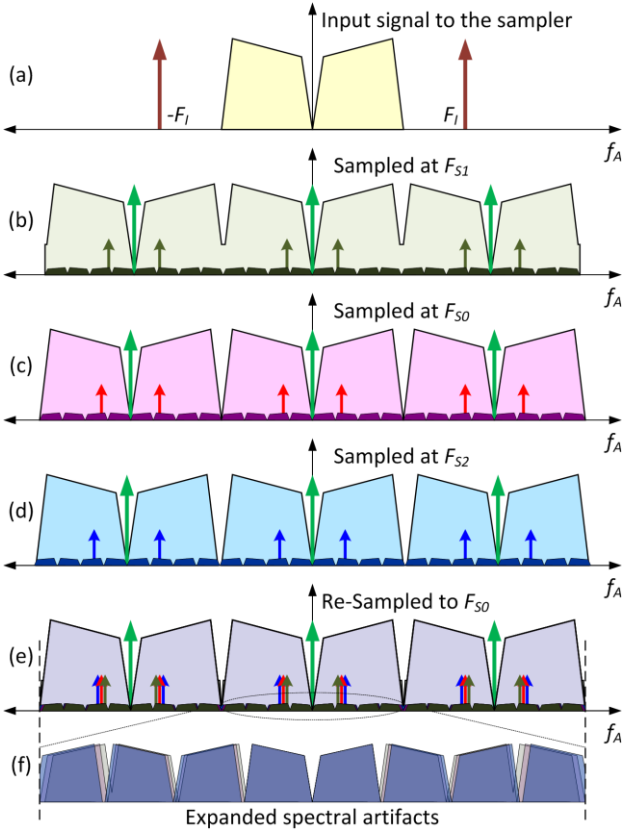


Figure 1 A sampling scenario with the SCFO scheme where the desired signal lies in Nyquist zone-1. The spectrum of the input (a) and spectra of the three sampled sequences sampled with the sample frequencies F_{S1} , F_{S0} and F_{S2} , (b), (c) and (d), respectively. The overlaid spectra of the sequences resampled to F_{S0} (e) and expanded spectral artifacts (f).

that the spectral distribution is drawn with respect to the ‘apparent-frequency’ (i.e. the equivalent frequency in Hz). In theory, for the sampled spectra the spectral components are within $[-0.5F_{Sn}, 0.5F_{Sn}]$; $n = 0, 1, 2$ are replicated infinitely but, for clarity just the three adjacent replications are shown in Figure 1-(b), (c) and (d). Because the sampling frequencies are different the aliased components of the out-of-band interferer and the spectral images due to clock spurs and gain/timing mismatches in time interleaved samplers appear at different apparent frequencies in each of the spectra except around $f_A = 0$. Note that the DC offset of the sampler maps to $f_A = 0$ and, for an interleaved sampler, it is possible that these multi-phase lower-rate clocks may also leak into the signal path (although not shown here).

According to the SCFO scheme, the sequences that are sampled at different sample-rates are digitally resampled into a common sample rate (i.e. F_{S0}) before correlation or beamforming. The spectra of the resampled sequences are overlaid and shown in Figure 1-(e). Note that the spectrum of the desired signal as well as the spectral components due to DC offsets of the sampler overlap as shown in Figure 1-(f) and will correlate. However, non-

spectral overlapping components don’t, with a diminishing decorrelation (i.e. fringe washing) effect near DC.

Similarly, a sampling scenario with the proposed SCFO scheme where the desired signal is in Nyquist zone-2 is illustrated in Figure 2. The spectrum of the input signal to the sampler that includes an out-of-band interferer is shown in Figure 2-(a). The spectrum with respect to the apparent frequency for the three corresponding sampled sequences sampled with the frequencies F_{S1} , F_{S0} and F_{S2} , are shown in Figure 2-(b), (c) and (d), respectively. Here too the aliased components of the out-of-band interferer and the spectral images due to clock spurs and gain/timing mismatches in time-interleaved samplers appear at different apparent frequencies in each of the spectra.

For a Nyquist zone-2 sampled signal, the resampling process requires an additional frequency shift that is equivalent to the frequency offset in order to realign the desired spectral components. The spectra of the resampled and realigned sequences are overlaid and shown in Figure 2-(e). Note that the spectral components of the desired signal overlap. However, the spectral components due to out of band interferers, DC offset and sample clock

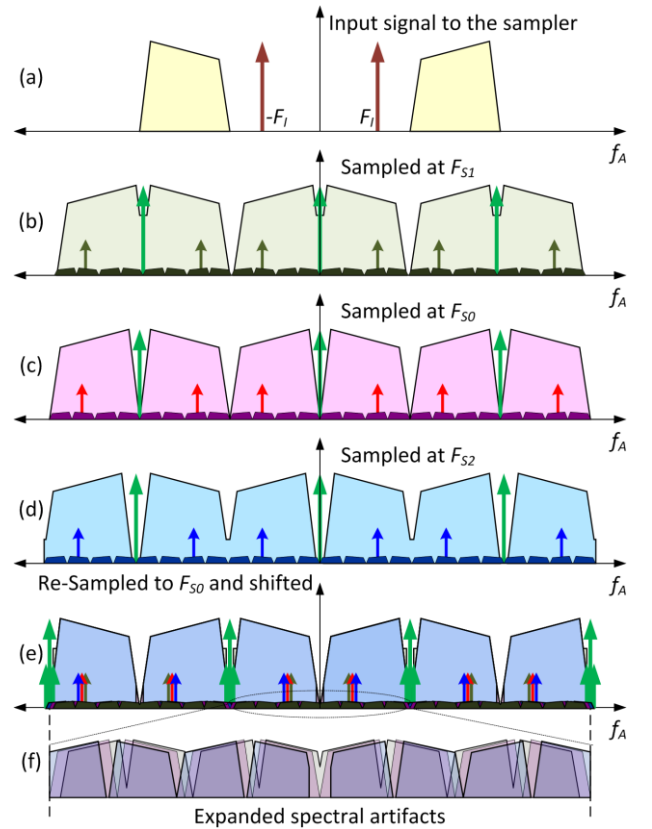


Figure 2 A sampling scenario with the SCFO scheme where the desired signal lies in Nyquist zone-2. The spectrum of the input (a) and spectra of the three sampled sequences sampled with frequencies F_{S1} , F_{S0} and F_{S2} , (b), (c) and (d), respectively. The overlaid spectrum of the sequences that are resampled to F_{S0} and re-aligned (e) and expanded spectral artifacts (f).

related spectral artifacts do not overlap as shown in Figure 2-(f). Hence, when cross-correlated the desired signals correlate; when added in a beamformer, the desired signals coherently add and the undesired spectral images and DC offsets don't correlate or coherently add.

4. The SCFO scheme in the SKA1 Mid Telescope Array: An Example

The implementation of the SCFO scheme in the SKA1 Mid Telescope array requires coordinated design among several elements of the telescope. In the proposed SCFO scheme, the Signal and Data Transport (SADT) element [1,2] must generate different clock frequencies F_{Sn} ; $n = 1, 2, \dots, N_{Sam}$ for all N_{Sam} samplers in the array. Preferably, these frequencies are specified in the form,

$$F_{Sn} = F_{S0} \pm n \cdot \Delta f; n = 1, 2, \dots, N_{Sam}, \quad (1).$$

where F_{S0} is the nominal sample frequency and Δf is the offset-frequency resolution that is proposed to be ~ 10 kHz. These different sampling frequencies are distributed by SADT to the antennas in DISH (DSH) element [1,2]. A *unique sampling frequency* is utilized in sampling each of the received signals from the antennas. In the CBF, the sampled data streams from the antennas are digitally resampled to a common sample rate using a real-time sample-by-sample fractional-delay filter-bank and a phase-modulator [6] Ch-06.

In order to empirically investigate the performance of the proposed SCFO scheme a simplified model of the SKA1 Mid telescope array signal processing has been developed. The model is fed with 3 pairs of noise-contaminated sequences containing a common bandlimited random signal of power σ_S^2 . The first pair $\{x_{R1}, x_{R2}\}$ consists of the ideally sampled common signal contaminated by two independent Gaussian noise sequences of power σ_N^2 . In the second pair $\{x_{D1}, x_{D2}\}$ the common signal is sampled with two non-ideal M -phase time-interleaved samplers at the common sampling frequency F_{S0} . The normalized gain and time mismatches of the two time-interleaved samplers are specified by $[2 \times M]$ matrices \mathbf{G} and \mathbf{T} , respectively [0]. The resulting two sampled sequences are also contaminated (before sampling) by two independent Gaussian noise sequences of power σ_N^2 . The third pair $\{x_{O1}, x_{O2}\}$ consists of the two sequences of the common signal sampled at F_{S1} , and F_{S2} , respectively, using the same non-ideal samplers and contaminated by two independent Gaussian noise sequences of power σ_N^2 . Subsequently, this pair of sequences is resampled into $\{x_{A1}, x_{A2}\}$ corresponding to the rate F_{S0} . The auto and cross correlations of the sequence pairs $\{x_{R1}, x_{R2}\}$, $\{x_{D1}, x_{D2}\}$ and $\{x_{A1}, x_{A2}\}$ are evaluated using a simple 512-lag XF correlator. Finally, the spectra of the auto correlations and cross correlations are evaluated.

A couple of simulations, one each for Nyquist zone-1 and 2 sampling, have been conducted in order to validate the

assumptions of the proposed SCFO scheme. Both simulations are conducted with $\sim 6 \times 10^8$ samples that corresponds to ~ 0.1 s integration time at $F_{S0} = 6000$ MHz. For the Nyquist zone-1 sampling case, the input to the ideal samplers consists of a common bandpass stationary signal spanning 900 – 1200 MHz. For the non-ideal samplers the input also includes a leaked out-of-band interferer at 5628 MHz. Note that the contaminating Gaussian noise has the same power of the common bandpass signal. For the two non-ideal 4-phase time-interleaved samplers,

$$\mathbf{G} = \begin{bmatrix} 1.0665 & 0.9092 & 1.0260 & 1.0191 \\ 1.1748 & 1.0425 & 0.9838 & 0.8726 \end{bmatrix}, \quad (2).$$

$$\mathbf{T} = \begin{bmatrix} 0.1396 & 0.1054 & 0.0137 & 0.2480 \\ 0.0441 & -0.093 & -0.088 & 0.0583 \end{bmatrix}. \quad (3).$$

If any of the sums along the rows of \mathbf{T} is non zero, then there is net time delay corresponding to that sampler that appears as phase shift in the cross correlation. The input to the SCFO scheme has been sampled at $F_{S1} = 5999.9$ MHz and $F_{S2} = 5980.3$ MHz, respectively.

The spectra of auto correlations $XX_{R1}, XX_{R2}, XX_{D1}, XX_{D2}, XX_{A1}$ and XX_{A2} are shown in Figure 3. As expected the spectral components of the out-of-band interfere appears at different frequency-bins for XX_{A1} and XX_{A2} . Also, as expected there are 4 clear images of the out-of-band-interference due to interleaved sampler non-idealities.

The spectra of cross correlations XY_{R1R2}, XY_{D1D2} and XY_{A1A2} are shown in Figure 4. Note that for XY_{D1D2} three of the images that are shown inside the red-circles appear quite prominently with respect to XY_{A1A2} . Hence, the SCFO scheme has significantly suppressed the undesired effects of sample clock-related interferences and spectral artifacts due to gain and time mismatches of time-interleaved samplers.

For the Nyquist zone-2 sampling case, the input to the ideal samplers consists of a bandpass stationary signal spanning 4800 – 5100 MHz. The selected bandwidth allows the observation of images of the input spectrum due to gain and time mismatches. For the non-ideal samplers the input includes a leaked out-of-band interferer at 372 MHz. Similarly the contaminating Gaussian noise has the same power of the common bandpass signal. For the two time-interleaved samplers,

$$\mathbf{G} = \begin{bmatrix} 0.9864 & 1.0697 & 0.9759 & 0.8038 \\ 1.0557 & 1.0673 & 0.8035 & 1.0924 \end{bmatrix}, \quad (4).$$

$$\mathbf{T} = \begin{bmatrix} 0.1654 & -0.012 & 0.1522 & -0.025 \\ 0.0176 & 0.1322 & -0.014 & -0.252 \end{bmatrix}. \quad (5).$$

Similar to the previous case, the input to the SCFO scheme has been sampled at $F_{S1} = 5999.9$ MHz and $F_{S2} = 5980.3$ MHz, respectively.

The spectra of auto correlations $XX_{R1}, XX_{R2}, XX_{D1}, XX_{D2}, XX_{A1}$ and XX_{A2} are shown in Figure 5. Here, the images of the bandpass signal (in red circles) are noticeable.

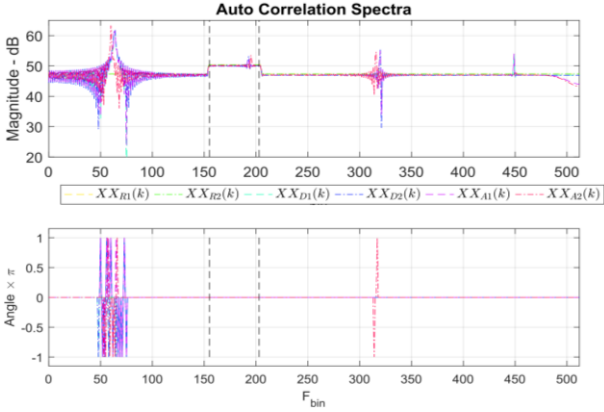


Figure 3 The magnitude (top) and phase (bottom) of the auto correlation spectra of XX_{R1} , XX_{R2} , XX_{D1} , XX_{D2} , XX_{A1} and XX_{A2} for Nyquist zone-1 sampling.

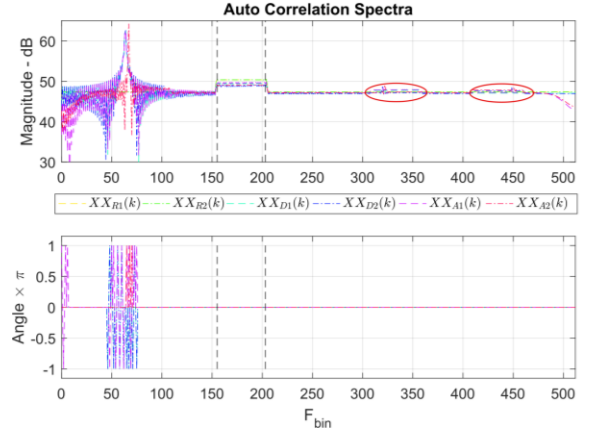


Figure 5 The magnitude (top) and phase (bottom) of the auto correlation spectra for Nyquist zone-2 sampling.

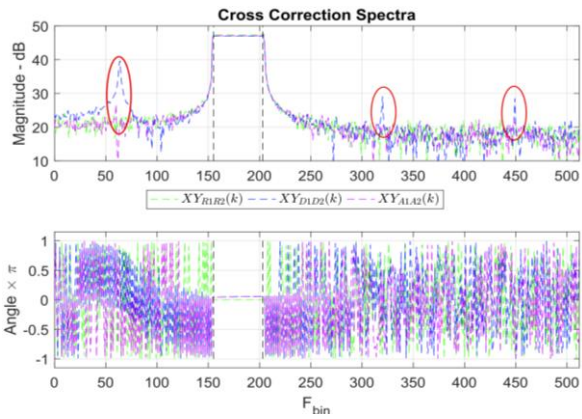


Figure 4 The magnitude (top) and phase (bottom) of the cross correlation spectra of XY_{R1R2} , XY_{D1D2} and XY_{A1A2} for Nyquist zone-1 sampling.

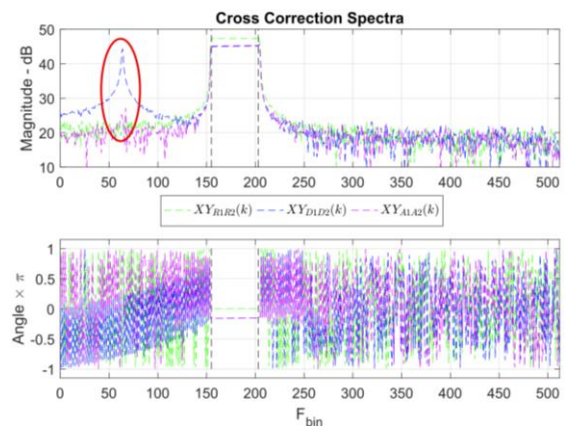


Figure 6 The magnitude (top) and phase (bottom) of the cross correlation spectra for Nyquist zone-2 sampling.

The spectra of cross XY_{R1R2} , XY_{D1D2} and XY_{A1A2} are shown in Figure 6. Note that for XY_{D1D2} just one of the images that is shown inside the red-circle appears prominently with respect to XY_{A1A2} . Also, note that the power of both XY_{D1D2} and XY_{A1A2} are about 2.5 dB less than that of XY_{R1R2} . This may be due to the power transferred to the spectral images of both XY_{D1D2} and XY_{A1A2} .

5. Conclusions

The SCFO scheme has been proposed for the SKA1 Mid telescope array in order to increase the spectral dynamic range of the observation in the presence of sample clock-related self-interference and out-of-band interference. The simulation results confirm that the proposed scheme can indeed suppress the spectral images due to gain and time mismatches of the time-interleaved samplers.

6. References

1. P. E. Dewdney, SKA1 SYSTEM BASELINE DESIGN (SKA-TEL-SKO-DD-001), Rev.-01, 2013-03-12. (Available online <https://www.skatelescope.org/key-documents/>)

2. P. E. Dewdney, SKA1 SYSTEM BASELINE V2 DESCRIPTION (SKA-TEL-SKO-0000308), Rev.-01, 2015-11-04. (Available online <https://www.skatelescope.org/key-documents/>)
3. T. Neu, "Impact of sampling-clock spurs on ADC performance," Analog Applications, 2009.
4. B. Razavi, "Problem of timing mismatch in interleaved ADCs," in *Proceedings of the IEEE 2012 Custom Integrated Circuits Conference*, 2012.
5. C. Vogel, S. Saleem, and S. Mendel, "Adaptive blind compensation of gain and timing mismatches in M-channel time-interleaved ADCs," in *2008 15th IEEE International Conference on Electronics, Circuits and Systems*, 2008, pp. 49–52.
6. F. J. Harris, *Multirate Signal Processing for Communication Systems*, Upper Saddle River, N.J: Prentice Hall, 2004.